Preparation and photocatalytic mechanism of graphene/ZnO composite photocatalyst

YUETING WANG[a], PEIMING ZHANG[b], SHANHONG LAN[a,*], CHAOPING WANG[b], SHANSHAN WANG[b], LINGYUN YE[a], SHIWEN GENG[d], HUIXIA LAN[b,c]

[a]*School of Environment and Civil Engineering, Dongguan University of Technology, Dongguan, 523808, China*

[b]*College of Environment and Safe Engineering, Qingdao University of Science & Technology, Qingdao,266042, China*

[c]*Fujian Provincial Key Laboratory of Ecology-Toxicological Effects & Control for Emerging Contaminants, Putian 351100, China*

[d]*Nouryon Chemicals(BoXing) Co., Ltd, Binzhou256500, China*

Different ratios of graphene/ZnO photocatalytic materials were successfully synthesized by solution mixing method. The synthesized samples were characterized by X-Ray Diffractomer (XRD), Scanning Electron Microscope (SEM) and Ultraviolet (UV) diffuse reflection. The best composite ratio was 1: 30 determined by sample characterization combined with photocatalytic degradation experiment. The reaction mechanism was speculated by the photocurrent density curve of graphene/ZnO and the photocatalytic degradation of Methyl Orange (MO) by graphene/ZnO in the presence of different capture agents, the results indicated that OH plays a main role in the photocatalytic reaction, while the positive hole has an auxiliary effect.

(Received September 11, 2019; accepted October 22, 2020)

Keywords: ZnO, Graphene, Composite, Photocatalysis

1. Introduction

Nowadays, the problem of water pollution is becoming more and more serious. Photocatalytic technology has attracted the attention of researchers as a green sewage treatment technology with high efficiency and environmental protection. As a typical photocatalytic material, ZnO has been widely used in the fields of optics and catalysis [1-3]. However, the photocatalytic efficiency of semiconductors is greatly affected by the yield of photogenerated electron-hole, the recombination rate of photogenerated electrons and holes directly determines the photocatalytic effect. Ahmadi et al. found that some hole-electron do not contribute to the photocatalytic process by studying the photocatalytic properties of $SrTiO_3$ [4]. In order to improve the photocatalytic efficiency of semiconductor material, researchers have found such methods as deposition of noble metals, recombination of semiconductors, doping of metal ions, etc.[5-12], can improve the photocatalytic activity of semiconductor oxide to a certain extent, but there is still a long distance from a large scale of production and application.

Graphene is a planar two-dimensional structure composed of a single layer of carbon atoms, each carbon atom is connected by sp2 hybridization, the angle between C-C is 120°, the bond length is about 0.142 nm, its bond energy is very strong and its structure is very stable [13-14]. Graphene has attracted great attention of researchers because of its good electrical conductivity [15], electron mobility [16], thermal conductivity [17], and large specific surface area [18]. It has also been widely used in the field of photocatalysis. Chen et al. studied the applications of four graphene semiconductor oxide composite photocatalysts and obtained good results [19]. Tang et al. used graphene/ZnO composites to treat methyl blue solution, and found that it can degrade methyl blue effectively [20]. Therefore, composite of graphene and ZnO which forms an electron interaction at the interface compensates for the shortcomings of ZnO by graphene, and reduces the combination of electrons and holes. In this paper, graphene /ZnO composites with different composite ratios were prepared by ultrasonic solution mixing method. XRD, SEM and other characterization were carried out, and the photocatalytic degradation performance of graphene /ZnO composites under visible light was studied. By studying the effects of capture agent on the catalytic degradation efficiency and stability of graphene/ZnO composites under visible light, the degradation mechanism of graphene/ZnO composites was further obtained.

2. Experimental materials and methods

2.1. Preparation of graphene/nanometer ZnO photocatalyst

Some amount of ZnO, 0.1g grapheme and 100mL deionized water were put into a 250ml beaker. The beaker was placed on a magnetic mixer and stirred vigorously for two hours, and then dispersed by Ultrasound. Finally, the mixture was rapidly heated and recombined, and various ratio of composites photocatalyst were obtained.

2.2. Characterization of graphene composite nanometer ZnO photocatalyst

X - ray diffractometer was used for slow scanning near the principal crystal angle of graphene/ZnO to obtain the phase composition of the sample and the structural information of graphene/ZnO. Scanning electron microscope (SEM, jsm-6700f, Japan) was used to observe the microscopic morphology, the surface structure and particle size of the samples. UV-2600 UV-visible diffuse reflectance spectrometer (Shimadu company of Japan) was used to determine the wavelength of light response of photocatalyst in the range of 200-800 nm. Barium sulfate powder was used as reference to measure the absorption spectrum of the substance and characterize the light response range of the sample by scanning the liquid and solid phases.

2.3. Evaluation of photocatalytic activity

The photocatalytic experimental device and process were according to the reference [21]. The dosage of graphene /ZnO was 0.2g, the concentration of methyl orange (MO) solution was 10mg/L, and the volume was 100ml. Photocatalytic degradation efficiency was characterized by decolorization rate. Removal rate $=(C_0-C)/C_0$, where C_0 and C are the concentrations of organic pollutants before and after treatment respectively, mg/L.

3. Results and discussion

3.1. Graphene composite nanometer ZnO photocatalyst characterization

The fixed ultrasonic power was 100W and the frequency was 60KHz. The XRD pattern of different composite ratios was shown in Fig. 1.

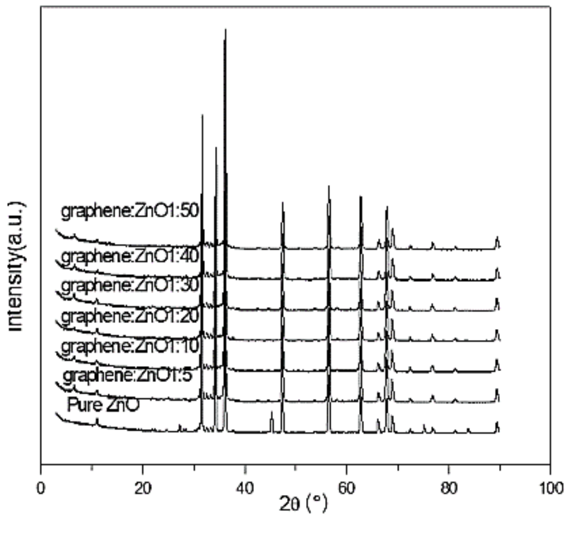

Fig. 1. XRD spectrum of graphene/ZnO composites with different composite ratios

From Fig. 1,we could see that graphene/ZnO XRD charts of different composite ratio were basically identical, the 2θvalues were 31.8°, 34.4°, 36.3°, 47.5°, 56.6°, 62.9° 68.1° and so on, corresponding to the ZnO hexagonal crystal plane of (100), (002), (101), (102), (110), (103) and (200) (JCPDS No. 89-0511), which were in line with standards card, belonging to the Hexagonal Fiber Mine. It indicated that the presence of graphene did not change the ZnO crystal form, and it didn’t destroy the structure of ZnO.

The SEM images of different composite ratios of graphene/ZnO were shown in Fig. 2.

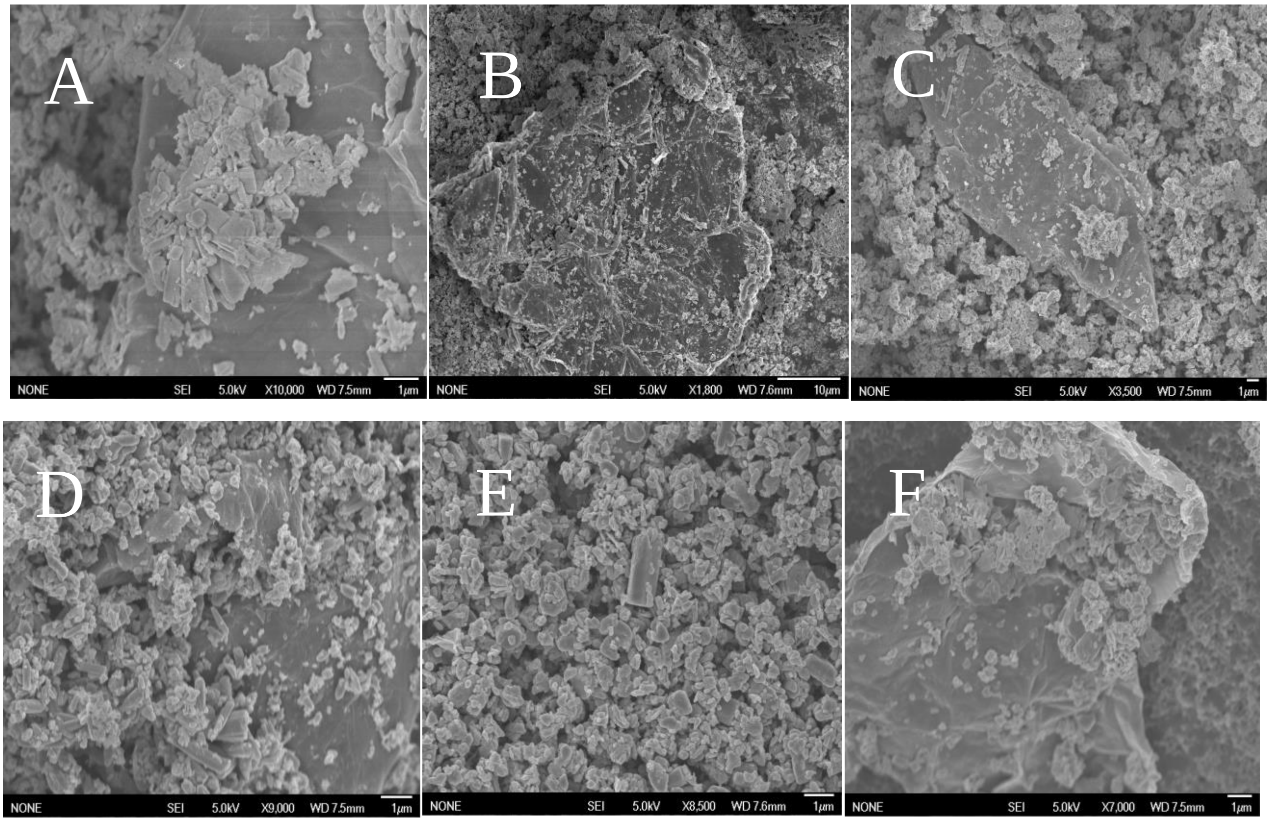

Fig. 2. SEM images of graphene/ZnO made in different composite ratios (A)graphene/ZnO 1 ∶5; (B)graphene/ZnO 1 ∶10; (C)graphene/ZnO 1 ∶20; (D)graphene/ZnO 1 ∶30; (E)graphene/ZnO 1 ∶40; (F)graphene/ZnO 1 ∶50

From Fig. 2, it can be seen that the composite proportion of graphene /ZnO had little effect on the structure and morphology of graphene, which indicated that graphene has good stability. When the graphene/ZnO composite ratio was 1:50, much ZnO agglomerated together on the surface of grapheme. The reason was that the amount of graphene was too little to provide enough oxygen-containing functional groups to bind to the active site of ZnO. Excess ZnO would agglomerate together as the decrease of the amount of graphene. When the composite ratio of graphene/ZnO increased to 1:30, graphene could bind well with ZnO and reduce the agglomeration of ZnO. We speculated that the reason was that with the increase of graphene content, the reductive functional groups of graphene increased, which could provide more sites to bind with ZnO, so that ZnO particles were not easily agglomerated with each other, and ZnO could be better spread on the surface of graphene. Sunil et al. synthesized graphene /ZnO composites by solvent-free method and was used to MB decolorization [22]. It was found that graphene would bind with the active site on ZnO, thus photocatalytic degradation could be carried out better.

Uv-visible diffuse reflectance spectra of graphene /ZnO with different composite proportions were shown in Fig. 3.

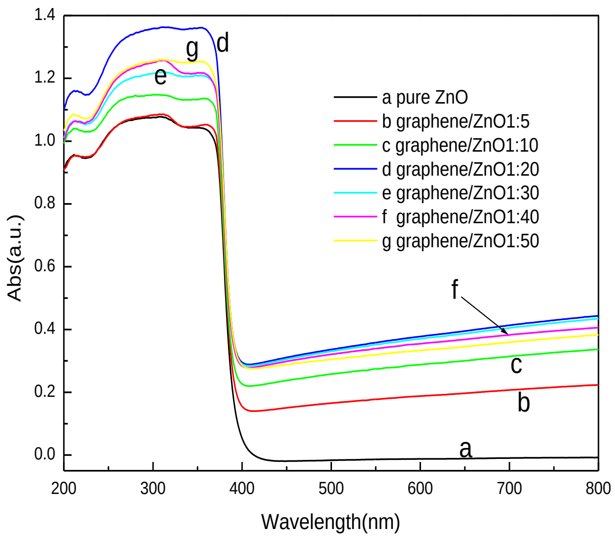

Fig. 3. UV-visible diffuse reflectance spectra of graphene/ZnO with different composite ratios (color online)

From Fig. 3, it could be seen that the absorption band edge of pure ZnO was about 380nm, which indicated that ZnO had good absorption in the ultraviolet region. Compared with the light absorption curve of pure ZnO, the absorption curve of the composites showed a slight red shift with the increase of the proportion of Graphene modified composites. And it was found that the presence of graphene could extend the light absorption region of ZnO to the range of visible light. In the wavelengths range larger than 400 nm in visible light region, the visible light absorption capacity of the sample was relatively strong when graphene/ZnO composite ratios were 1:20 and 1:30. But when the proportion of ZnO/graphene composite reduced to 1:40, the light absorption capacity of the composite material decreased. It meant that within a certain composite ratio, the addition of graphene increased absorption of the visible light by graphene/ZnO, which had a certain significance for the research on the photocatalytic degradation performance of graphene/ZnO under the condition of visible light. Wen et al. it was found that the formation of Ti-O-C bond narrowed the P25energy gap by the synthesis of p25-rGO composite materialand the absorption of visible lightbecomed strong,which was consistent with the research results in this study [23].

3.2. The photocatalytic degradation performance of graphene/ZnO with different composite ratios

Photocatalytic performance of graphene/ZnO with different composite ratios in MO solution was shown in Fig. 4.

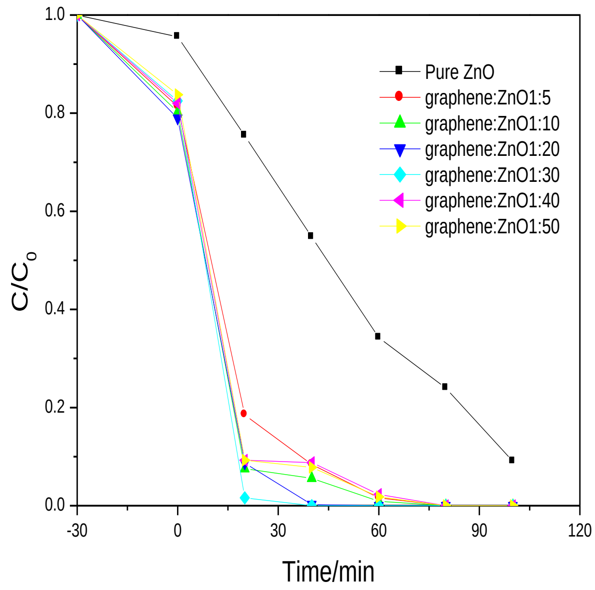

Fig. 4. Photocatalytic degradation of graphene/ZnO with different composite ratios in MO solution (color online)

It could be seen from Fig. 4, the photocatalytic performance of graphene/ZnO was better than that of pure ZnO in visible light region after 30 min absorption in dark state. MO was completely decomposed in 30 min. Appropriate amount of graphene was beneficial to improve the photocatalytic performance of graphene/ZnO. However, as the content of graphene increased, the inhibition of the photocatalytic degradation performance of graphene/ZnO occurred. The reason could be that within a certain range of composite ratio, as the increase of graphene/ZnO ratio, the electric charge was rapidly transported and effectively separated by the role of graphene. Therefore, electrons in ZnO excited by visible light could be rapidly transferred through graphene, and the recombination of electrons and holes was effectively avoided. Thus, graphene/ZnO could show the best visible light catalytic degradation ability when its composite ratio was 1:30.

3.3. The photocatalytic mechanism of graphene/ZnO composites

When the ratio of graphene /ZnO was 1:30, the photo induced current density curves of graphene /ZnO were shown in Fig. 5.

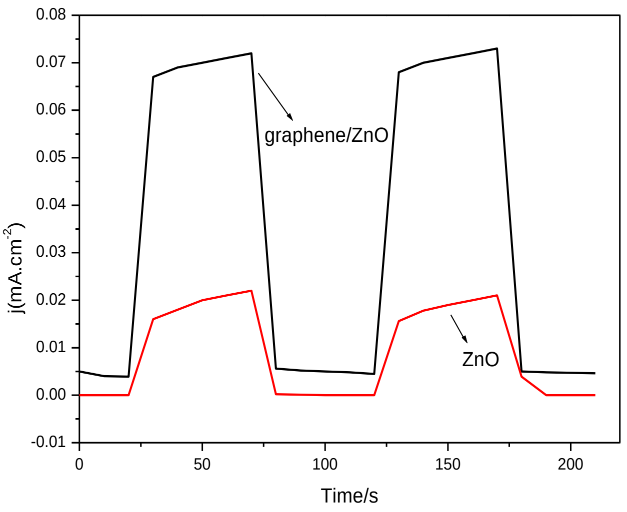

Fig. 5. Photoinduced current density curves of graphene/ZnO photocatalysts (color online)

It could be seen from Fig. 5, during each switching on and off of the two electrodes, photocurrent transients had almost the same shape for each electrode, because of the role of ZnO. For the photoinduced current density curve of ZnO, when the light irradiation was ceased, the photocurrent decreased back to zero. It was worth noticing that the photocurrent of the graphene/ZnO electrode was 0.07mA·cm^{-2}, while the photocurrent of the ZnO electrode was about 0.02 mA·cm^{-2}. The photocurrent of the graphene /ZnO electrode was about 3.5 times that of the ZnO electrode, which indicated that the photocatalytic degradation of MO solution bygraphene /ZnO in visible light region mainly relied on the separation efficiency of photo-induced carriers accelerated by graphene. Moreover, graphene played a good role in electron transport, which greatly reduced the possibility of the recombination of photogenerated electrons and holes.

Photocatalytic degradation of MO by graphene /ZnO in the presence of different capture agents were shown in Fig. 6.

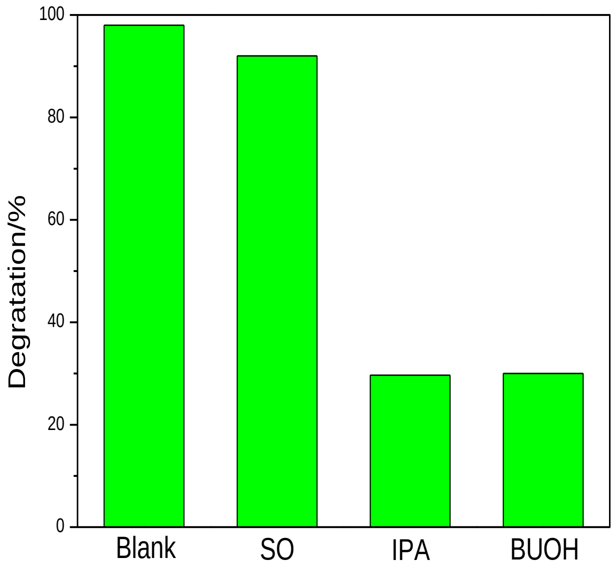

Fig. 6. Effects of different free-radical scavengers on degradation of MO by graphene/ZnO under visible light irradiation (color online)

We could see from Fig. 6 that MO solution can achieve 98% degradation in 60 minutes under visible light irradiation, when 50mmol/L sodium oxalate (SO) was added, 92% of MO could be degraded by graphene /ZnO in 60min under visible light irradiation. It indicated that hole was not the main active substance in determining photocatalytic reaction. However, when added 50mmol/L n-butanol (BUOH) and isopropanol (IPA), the degradation efficiency of MO decreased rapidly. It could be seen from the figure, after added two capture agents, only 30.2% and 29.1% of MO removal rates achieved by graphene /ZnO under visible light at 60 min, respectively. It suggested that OH·produced by photogeneration electrons was the main active substance to affect photocatalytic performance of graphene/ZnO. In conclusion, the combined actionof photogenic holes and OH·generated by photogenic electrons affected photocatalytic degradation of MO solutionby graphene /ZnO in the visible light. The results were consistent with that of Wang et al. [24].

The mechanism of photocatalytic degradation of MO by graphene/ZnO was shown in Fig. 7.

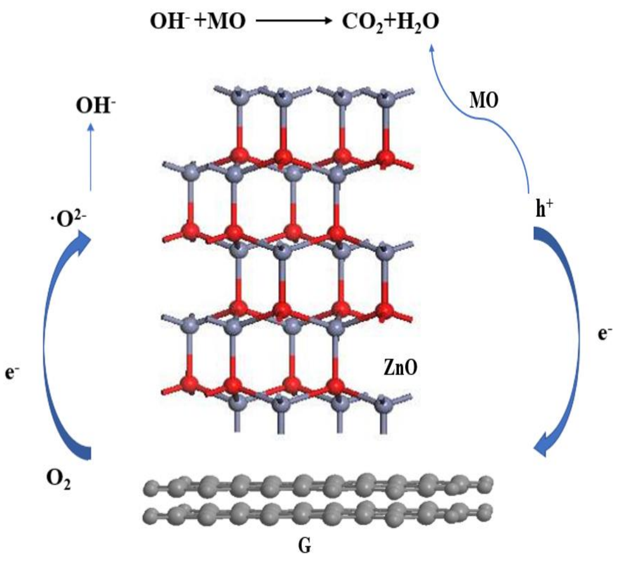

Fig. 7. Photocatalytic mechanism of graphene/ZnO photocatalyst for MO degradation (color online)

Graphene had good stability. Under different pH conditions, graphene could protect ZnO well, inhibitining the corrosion of ZnO to a certain extent, and improve the stability and reusability of ZnO[21].In addition, graphene had high electrical conductivity, and the carrier mobility of graphene at room temperature could generally reach $15000cm^2.v^{-1}.s^{-1}$. For graphene/ZnO system, when ZnO and graphene composited in different Fermi level , which would form a schottky barrier, in general, electrons would transfer from graphene (which was higher in Fermi) to ZnO (which was lower in Fermi), electronic e^- moved to the ZnO. As electron capture devices, ZnO inhibitedthe recombination of electron and hole, and the photocatalytic performance improved. But in this system, when the graphene and ZnO composited, the photogenic electrons generated from ZnO excited by visible light could be quickly transferred to the graphene surface, that was because plasma resonance effect occured in ZnO photoinduced excitation,it might lead to inter-band excitation and high energy electrons that could overcome the schottky barrier and transfer to graphene,the e^- transferred to the surface of graphene could combine with dissolved oxygen in the solution to form a highly reductive $\cdot O^{2-}$, thus, the hole h^+ in the valence band was not easy to recombine with the electron. The flat band potentials of ZnO and graphene /ZnO were -0.36 V and -0.29 V, respectively. The electrochemical impedance spectroscopy (EIS) Nynquist arc radius of the graphene /ZnO electrode was much smaller than that of the ZnO electrode[25],indicated that the presence of graphene could accelerate the separation of electrons and holes.

4. Conclusions

(1) The graphene/ZnO composites in different composite ratios were successfully prepared, and the best composite ratio of graphene / ZnO was determined as 1:30 through XRD, SEM, UV-visible diffuse reflection and photocatalytic degradation experiments.

(2) The photo-induced current density of graphene/ZnO electrode was as 3.5 times as the pure ZnO electrode, indicated that graphene played an important role in electron transfer in MO photodegradation by graphene/ZnO under visible light.

(3) The combined roles of photo-generated holes and OH· were important to the decomposition of MO, and the presence of graphene could effectively inhibit the recombination of photogenerated electron-hole pairs and improve the photocatalytic efficiency.

Acknowledgments

The authors are grateful for the support of Fujian Provincial Key Laboratory of Ecology-Toxicological Effects & Control for Emerging Contaminants (PY18002).

References

[1] S. Li, P. Wang, R. Wang, Y. Liu, R. Jing, Z. Li, Z. Meng, Y. Liu, Q. Zhang, Applied Surface Science **497**, 143682 (2019).
[2] Z. Li, X. Fan, A.Meng,Y. Zhang, K. Zhu, Q. Li, Journal of nanoscience and nanotechnology **19**(11), 7163 (2019).
[3] W. Yu, J. Zhang, T. Peng, Applied Catalysis B, Environmental **181**(12), 220 (2016).
[4] M. Ahmadi, M. S. Seyed Dorraji, M. H. Rasoulifard, A. R. Amani-Ghadim, Separation and Purification Technology **228**(12), 115771 (2019).

[5] K. Alamelu, V. Raja, L. Shiamala, B. M. J. Ali, Applied Surface Science **430**(2), 145 (2018).
[6] P. Jing, X. Zhou, J. Zhong, J. Hu, Physics Letters **383**(31), 125883 (2019).
[7] J. Shi, G. Xu, L. Miao, X. Xu, Journal of physical chemistry **27**(6), 1287 (2011).
[8] L. H. Lee, W. C. Chen, Chemistry of materials **13**(3), 1137 (2001).
[9] J. Lang, Q. Zhang, Q. Han, Y. Fang, J. Wang, X. Li, Y. Liu, D. Wang, J. Yang, Materials Chemistry and Physics **194**(6), 29 (2017).
[10] H. Zhang, W. Li, G. Qin, H. Ruan, Z. Huang, F. Wu, C. Kong, L. Fang, Applied Surface Science **492**(10), 392 (2019).
[11] H. Luitel, P. Chettri, A. Tiwari, D. Sanyal, Materials Research Bulletin **110**(2), 13(2019).
[12] D. Pugliese, F. Bella, V. Cauda , A. Lamberti, A. Sacco, E. Tresso, S. Bianco, ACS Applied Materials & Interfaces **5**(21), 11288 (2013).
[13] A. K. Geim, K.S. Novoselov, Nat. Mater **6**(3), 183 (2007).
[14] K. S. Novoselov, A. K. Geim, S. V. Morozov, D. Jiang, M. I. Katsnelson, I. V. Grigorieva, S. V. Dubonos, A. A. Firsov, Nature **438**, 197 (2005).
[15] N. Zhang, M. Q. Yang, S. Liu, Y. Sun, Y. J. Xu, Chemical reviews **115**(18), 10307 (2015).
[16] K. S. Novoselov, A. K.Geim, S. V. Morozov, D. Jiang, Y. Zhang, S. V. Dubonos, I.V. Grigorieva, A. A. Firsov, Science **306**, 666 (2004).
[17] N. J. Song, C. Ma, Materials **12**(12), 2030 (2019).
[18] H. Z. Chen, Chinese Science Bulletin **57**(23), 3000 (2012).
[19] J. Chen, J. Shi, X. Wang, H. Cui, M. Fu, Chinese Journal of Catalysis **34**(4), 621 (2013).
[20] X. Zhu, Y. Meng, Plating and Finishing **41**(07), 20 (2019).
[21] S. Lan, H. Zhang, J. Hu, S. Geng, H. Lan, J. Optoelectron. Adv. M. **20**(5), 337 (2018).
[22] P. L. Sunil, P. Vishnu, A. Ahmed, Applied Surface Science **465**(1), 1107 (2018).
[23] H. Wen, Y. Long, W. Han, W. Wu, Y. Yang, J. Ma, Applied Catalysis A: General **549**, 237 (2018).
[24] L. Wang, Z. Li, J. Chen, Y. Huang, H. Zhang, H. Qiu, Environmental pollution **249**(01), 801 (2019).
[25] G. Williams, P. V. Kamat, Langmuir **25**(24), 13869 (2009).

*Corresponding author: lllssshhhh@126.com